International Journal of Mass Spectrometry and Ion Processes, 105 (1991) 129–145
Elsevier Science Publishers B.V., Amsterdam

A PULSED ION BOMBARDMENT TIME-OF-FLIGHT MASS SPECTROMETER WITH HIGH SENSITIVITY FOR THE ANALYSIS OF PEPTIDES

VISWANATHAM KATTA and BRIAN T. CHAIT
The Rockefeller University, 1230 York Avenue, New York, NY 10021 - 6399 (U.S.A.)
(Received 10 September 1990)

ABSTRACT

The design and performance of a pulsed ion bombardment time-of-flight mass spectrometer that has an optimum sensitivity in the low picomole range for peptides is described. High sensitivity is achieved by efficient utilization of the sample introduced into the mass spectrometer. The peptide sample is concentrated on a small surface area (composed of nitrocellulose) and bombarded with a sufficiently intense, tightly focussed (elliptical spot with major axis of 0.12 mm) primary beam of indium ions (30 keV energy produced by a liquid metal ion source) to utilize a large proportion of the sample. The resolution of the instrument was limited (about 1000 FWHM) by the requirement that the secondary ion energy be less than 3.5 keV. High quality mass spectra were obtained from picomole amounts of peptides with molecular masses ranging up to 6000 u, in times of 3–30 min.

INTRODUCTION

The mass spectra of peptides can be measured at high sensitivities with ion bombardment time-of-flight (TOF) mass spectrometry [1–3]. These high sensitivities result from the ability of ion bombardment to produce significant amounts of quasi-molecular ions from peptides and the high efficiency of TOF mass analyzers. The bombarding ions can be of high energy (ca. 100 MeV), usually fission fragments produced during radioactive decay of ^{252}Cf, or of low energy (5–40 keV) produced, for example, from a thermionic alkali metal ion source. In both energy regimes, samples are prepared as thin solid layers electrosprayed on metal backings [4] or adsorbed to metallic [5,6] or polymeric [7,8] surfaces. To achieve the highest possible sensitivities, it is necessary to make full use of the sample inserted into the mass spectrometer.

Full use of the sample is impractical with fission fragments because it is difficult to obtain a sufficiently high flux density (very intense ^{252}Cf sources are hazardous) and to focus these high energy ions. To maximize the flux of fission fragments through the sample, it proves necessary to arrange the sample such that it subtends a large solid angle at the ^{252}Cf source. This is

0168-1176/91/$03.50

generally achieved by placing the sample in close proximity to the source and by depositing the sample over a relatively large area (ca. 1 cm^2) *. To maximize the secondary ion yield, it is also necessary to provide complete coverage of this large area with sample molecules, requiring considerable quantities of sample ($> 100\,pmol\,cm^{-2}$). However, because fission fragment flux densities are low (a few thousand $cm^{-2}\,s^{-1}$), only a small fraction of this sample is actually consumed in producing the mass spectrum (typically $< 0.01\%$). This inefficient use of the sample limits the effective sensitivity and speed of ^{252}Cf plasma desorption mass spectrometry.

In our own studies of some two thousand different peptides conducted over the past ten years [9], we have frequently found it necessary to accumulate ^{252}Cf plasma desorption mass spectra for periods extending up to several hours, especially when the available quantity of sample was less than 10 pmol. Motivated by a desire to reduce these accumulation times and to increase the sensitivity, we began, several years ago, to explore the potential of kiloelectronvolt energy ion bombardment TOF mass spectrometry for the measurement of peptides [10]. Although the desorption efficiencies of peptides by kiloelectronvolt ions are smaller than those by fission fragments [11–13], high fluxes of kiloelectronvolt ions can be readily focussed to a spot of small dimensions [10,14,15]. Thus, high sensitivities can be achieved by concentrating the sample on a small area and bombarding it with a sufficiently intense, tightly focussed kiloelectronvolt energy ion beam to utilize the entire sample.

We have designed and constructed a pulsed ion bombardment time-of-flight mass spectrometer that utilizes the above described principle [10,15]. The performance of the instrument was determined by measuring the mass spectra of peptides with molecular masses ranging up to 6000 u, deposited on thin nitrocellulose layers on a sample probe tip with a small area. The optimum mass spectrometric response was found for peptide amounts in the range 1–2 pmol. We report here the detailed design and performance of this mass spectrometer.

MASS SPECTROMETER—OVERALL DESIGN

The design of the present TOF mass spectrometer (Fig. 1) is similar to the instrument reported earlier by Chait and Standing [14], but with some significant differences. We will describe first the overall design of the present instrument and then discuss the details of the design with an emphasis on those features that differ from the earlier instrument.

The mass spectrometer shown schematically in Fig. 1 consists of a pulsed primary ion source, and a time-of-flight mass analyzer. Primary ions (In^+)

* Recently Macfarlane and co-workers have been using small area samples in ^{252}Cf plasma desorption mass spectrometry.

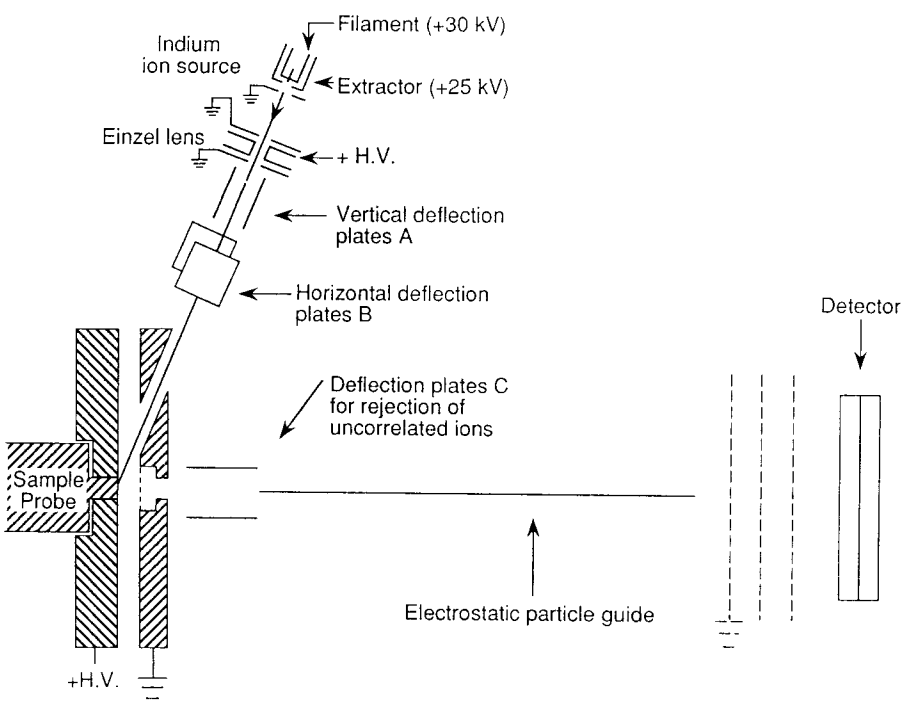

Fig. 1. Schematic representation of the pulsed ion bombardment time-of-flight mass spectrometer (not to scale).

with an energy of 30 keV are produced by an electrohydrodynamic liquid metal ion source and are focussed by an einzel lens so that they pass through a 2 mm diameter hole in a gridded secondary ion acceleration electrode and strike the sample probe tip (cylindrical rod, diameter = 2 mm). Because of the large angle of incidence (70°), the shape of the beam spot on the probe tip is elliptical with the length of the major axis being 0.12 mm. A short duration burst of primary ions is produced at the sample probe surface by the application of a fast risetime, high voltage pulse to one of a pair of deflection plates (plates A in Fig. 1). The high voltage deflection pulse causes the focussed beam spot to sweep rapidly upwards across the flat surface of the 2 mm diameter sample probe tip. Secondary sample ions are emitted from the probe tip during the short time interval (a few nanoseconds) in which the primary ion beam sweeps across its face. The leading edge of the high voltage deflection pulse provides a zero time reference point for the production of sample ions.

The probe tip fits into a small metal plate (Fig. 1) to make up an extended flat surface that provides a uniform accelerating field between the sample and the gridded acceleration electrode. The acceleration field is directed along the

axis of the flight tube. Secondary ions (mass m_s, charge q_s) produced from the sample at a potential V_s relative to the grounded gridded electrode are accelerated to an energy $q_s V_s$ and pass into the flight tube. A 2 mm diameter collimator in close proximity to the grid electrode removes secondary ions produced from regions other than the sample probe tip. An electrostatic particle guide [16] compensates for radial divergence of the seondary ions, thereby increasing their transmission through the 2 m long flight tube. Secondary ions with different masses acquire different velocities, $v_s = (2q_s V_s/m_s)^{1/2}$, during acceleration; separate in space during flight; and reach the detector at the end of the flight tube at different times.

After each bunch of primary ions strike the sample probe, the time interval between the production of ions at the sample and their arrival at the detector is measured by a multistop time-to-digital convertor. These measured time intervals are rapidly transferred to the memory of a PDP 11/45 computer where they are stored in the form of a histogram of intensities versus time intervals (times-of-flight). The primary ion beam is pulsed at a rate of 2 kHz and the above sequence of events is repeated 2000 times per second; data are collected until sufficient statistics are accumulated.

PRIMARY ION SOURCE

In the present instrument an electrohydrodynamic liquid metal ion source [17] was chosen over the Cs^+ ion source used in the earlier design [14], for its higher brightness and also for its ability to generate high mass multiply charged cluster ions (a feature not discussed here). The metal, indium, was chosen for its low melting point (156°C) and low vapor pressure at the melting point. The ion source was fabricated in our laboratory using a method similar to that described by Wagner and Hall [17]. The source consists of a fine tungsten needle, with a radius of curvature of 3–4 micron at the electropolished tip, attached to a tungsten wire loop filament. The needle and part of the loop assembly are dipped into molten indium and removed in such a way that the needle is coated with indium and a small amount of indium is trapped in the loop assembly. This trapped indium serves as a reservoir giving a long life (> 100 h) to the source. The dipping operation is carried out under vacuum conditions to prevent oxidation of the indium and tungsten. In order to obtain stable emission, it is necessary to ensure that the indium fully wets the tungsten tip. This requires that any oxide layer on the tungsten surface be completely removed before it is dipped into the indium. The oxide layer can be effectively removed by heating the tip to a temperature of 1700°C in vacuum. Under the vacuum conditions used in our source preparation setup (1×10^{-6} Torr), it proved important to dip the fully heated tip into the molten indium reservoir. If the tip was allowed to cool before dipping, the

rapid formation of a surface oxide layer prevented the complete wetting of the tungsten.

In the mass spectrometer, the tungsten filament is biased at + 30 kV relative to ground and the indium is maintained just above its melting point by resistively heating the filament. An extraction electrode, containing a 1.8 mm diameter circular aperture and positioned 1 mm from the filament tip, is maintained a few kilovolts below the potential of the filament (Fig. 1). The strong electric field generated at the tip results in the emission of indium ions [18]. The emission is sustained by a continuous supply of molten indium to the tip from the reservoir. There is a threshold for the extracting field at which the emission begins to occur. At extracting fields higher than this threshold, stable emission currents of 1–50 μA are readily obtained. The acceleration of the primary ion beam is made in two steps. The first occurs between the emitting tip and the extraction electrode (potential difference of $\approx$ 5 kV) and the second between the extraction electrode and a grounded acceleration electrode containing a 2 mm diameter circular aperture situated 10 mm downstream (potential difference of $\approx$ 25 kV) (Fig. 1). The ion beam emanating from the extraction electrode has a large divergence. Although the second axial acceleration step reduces this divergence considerably, the beam striking the grounded acceleration electrode is sufficiently large ($\approx$ 5 mm) so that no steering is needed to transmit the beam into the next step of the optical system.

The ion beam is focussed on the sample probe plane to a spot of about 120 micron in diameter by a gridded einzel lens [14]. The beam is made to sweep upwards across the sample probe face by the application of a 1200 V amplitude, 8 ns risetime, 30 μs width pulse* to the "vertical" deflection plates, A (Fig. 1). Secondary sample ions are emitted from the sample tip during the short interval in which the ion beam sweeps across its face. The leading edge of this high voltage pulse also provides a time reference point, t_0, from which the flight time of ions produced from the sample is measured. At the end of the 30 μs wide high voltage pulse, the beam starts to return to its original position. To prevent the indium beam from restriking the sample during this retrace, another high voltage pulse (1020 V amplitude, 15 ns risteime, 30 μs width) is applied to the orthogonally oriented "horizontal" deflection plates, B, after a delay of 28 μs with respect to t_0. The electronic setup for pulsing the primary ion beam, detection of secondary ions, and flight time measurement is shown schematically in Fig. 2, and the timing sequence of these events is given in Fig. 3. The time interval measurements are made between the leading edge of the pulse applied to the "vertical" deflection plate, A, and the subsequent arrival times of secondary ions at the detector. The actual times-

* A Motorola MJ 16004 transistor was used in the avalanche mode to provide the high voltage pulses.

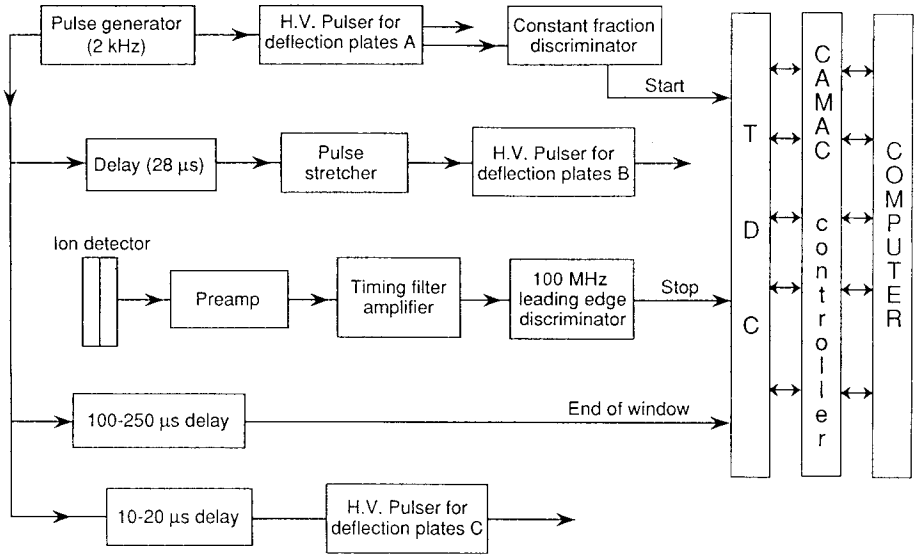

Fig. 2. Block diagram of the electronic setup used for pulsing the primary ion beam, for detecting the secondary ions, and for measuring their flight times with a TDC.

of-flight of the ions are, therefore, shorter than these measured intervals by the time taken for the primary In^+ ions to travel from the deflection plates to the sample probe (ca. 1100 ns).

The duration, Δt, of the burst of secondary ions emitted from the sample probe is determined by the length of time taken by the primary ion beam to sweep across the face of the 2 mm diameter probe tip. To a good approximation this time is given by

$$\Delta t = [(2m_p E_p)]^{1/2}\, d/eV_0 l]\, w \cos\theta_0 - [m_p/2E_p]^{1/2}\, w \sin\theta_0 \qquad (1)$$

where V_0 is the amplitude of the step wave form applied to the "vertical" plates A, d is the gap between the deflection plates, m_p is the mass of the primary ions, E_p is the energy of the primary ions, l is the distance of the deflection plates from the sample probe tip, w is the diameter of the sample probe tip, and θ_0 is the angle of incidence of the primary ion beam at the accelerating electrode.

The geometry of the primary ion beam interaction with the sample probe and the direction of the ion sweep is shown in Fig. 4. It is assumed that the two beam paths shown at the entrance of the aperture in the accelerating electrode are parallel and that the lens effect caused by this aperture is negligible. The first term of eqn. 1 accounts for the time needed to deflect the ion beam through a distance $w \cos\theta_0$ on a plane orthogonal to the beam axis [19]. During this deflection, the beam passes from the lowest extremity of the

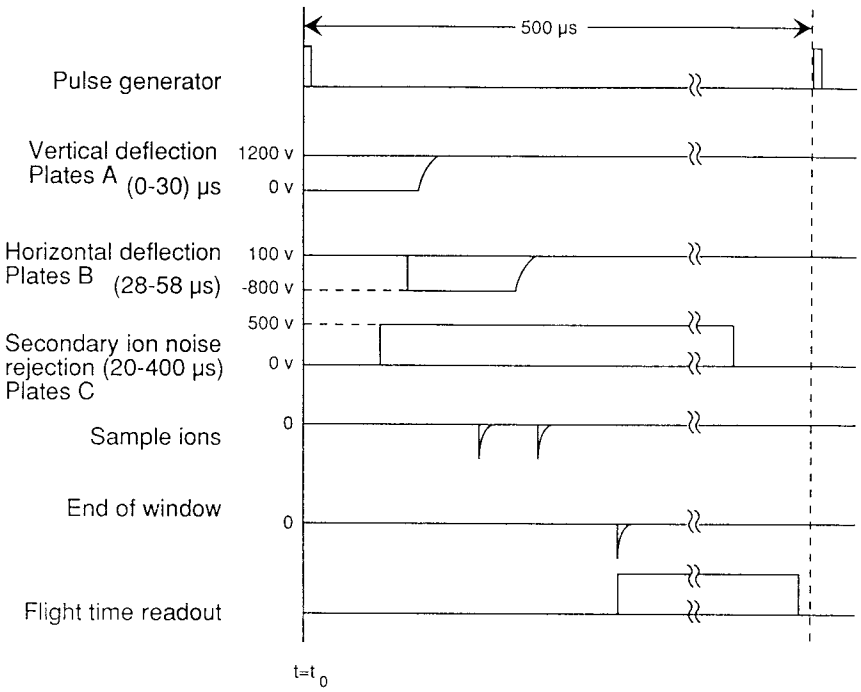

Fig. 3. Sequence of events occurring in each timing cycle. This sequence is repeated at a rate of 2000 times per second.

sample to the uppermost extremity. The second term accounts for the difference in primary ion flight times between the deflection plates and the upper and lower extremities of the sample probe tip resulting from differences in flight pathlengths. Since the two terms of eqn. 1 are opposite in sign, Δt can be made short by arranging for them to cancel exactly. This arrangement, which has been called angular time bunching [20], allows for all points on the surface of the sample swept by the beam to be struck simultaneously, at least in principle. Inserting the parameters used in the present setup ($V_0 = 1200\,\mathrm{V}$; $d = 1\,\mathrm{cm}$; $l = 25\,\mathrm{cm}$; $\theta_0 = 70°$; $E_p = 30\,\mathrm{keV}$; $m_p = 115\,\mathrm{u}$) into eqn. 1 gives a theroretical $\Delta t = 2.3\,\mathrm{ns}$.

Secondary ions are extracted from the sample into the flight tube by an electric field between the sample probe surface, maintained at a potential $-V_s$, and a grounded semi-transparent grid electrode (70% transmission). Primary ions passing through this acceleration field en route to the sample are deflected from their original trajectory so that [21]

$$\sin^2\theta/\sin^2\theta_0 = V_p/(V_p - V_s) \qquad (2)$$

where θ is the angle of incidence of the primary ion beam at the sample surface, θ_0 is the angle of incidence of the primary ion beam prior to entering

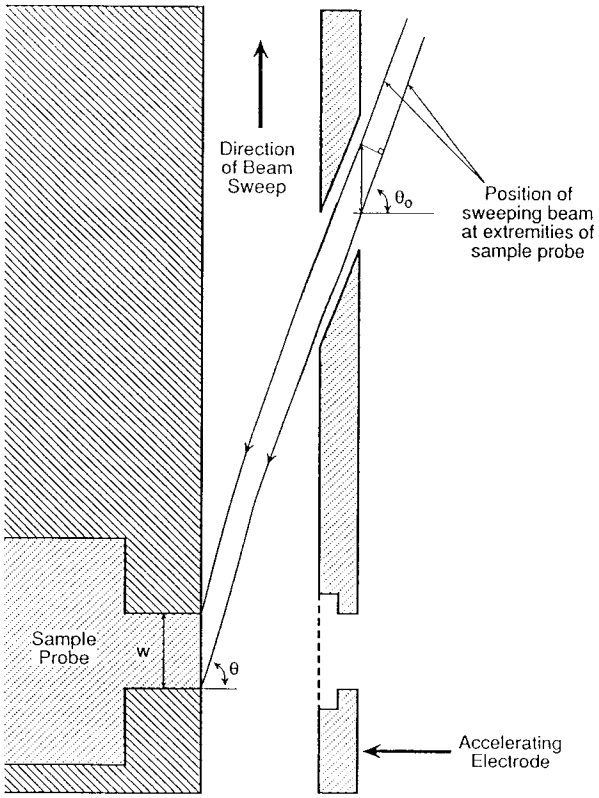

Fig. 4. Geometry of the interaction of the primary ion beam with the sample probe tip. The beam is swept upward with each high voltage pulse applied to the "vertical" deflection plates.

the secondary ion acceleration field, V_p is the potential applied to the primary ion filament, and V_s is the potential applied to the sample probe.

In the present apparatus, θ_0 is fixed at 70° and V_p at 30 kV. Insertion of these values into eqn. 2 shows, for positive secondary ions, that there is a maximum acceleration voltage (V_s = 3.5 kV) beyond which the ion beam is deflected through an angle large enough that it no longer strikes the sample. The positive ion acceleration potential, V_s, was therefore limited to 3.0 kV in all the investigations described here. For this value of the acceleration potential, the angle of incidence of the primary ion beam at the sample surface, θ, is 82° and the energy is 27 keV. The earlier instrument [14] utilized a more acute bombardment angle (θ_0 = 20° compared to 70° in the present design). This low angle of incidence allowed the use of considerably higher secondary ion acceleration potentials.

ION DETECTION AND FLIGHT TIME MEASUREMENT

Secondary ions are detected at the end of the flight tube by a pair of microchannel electron multiplier plates arranged in a chevron configuration and operated at gains compatible with single ion counting. A postacceleration potential of 7.5 kV at the detector increases the detection efficiency for high mass ions (total energy = q_s (3.0 + 7.5) keV).

The "start" pulse for the measurement of secondary ion flight times is generated by direct pickoff from the high voltage deflection pulse and feeding of the resulting signal into a fast timing discriminator (model 463, ORTEC, Oak Ridge, TN) (Fig. 2). Secondary ions striking the electron multiplier produce signals that are amplified (ORTEC model 9301 preamplifier and model 454 timing filter amplifier) and fed into a fast timing discriminator (ORTEC model 436) to produce "stop" pulses. The time-to-digital converter (TDC) (model 4208, LeCroy, Chestnut Ridge, NY; resolution = 1 ns) can measure eight such "stop" times once the TDC is armed by the "start" pulse. This means that up to eight secondary ions can be detected and their flight times measured for each primary ion pulse. The TDC is disarmed by an "end-of-window" pulse generated by a fixed delay, 100–250 μs after the "start" pulse. A CAMAC controller (model 3920, Kinetic Systems Corp., Lockport, IL) transfers the flight times from the TDC to the memory of a PDP 11/45 computer (Digital Equipment Corp., Maynard, MA). A period of 30 μs is required for transferring each flight time to the computer. After reading all the times from the TDC, the computer generates a signal that initializes the TDC for another cycle of "start" and "stop" pulses. This process is repeated 2000 times per second. Each digitized time the computer receives corresponds to an element in an array in the computer memory. When a measured time is received, the value of the appropriate element in the array is increased by one. The available memory of the 16-bit PDP 11/45 computer limited the array size to 18 000 elements. In order to scan to 180 μs (m/z 5000) the time channels thus have to be 10 ns wide and the full 1 ns resolution from the TDC cannot be used. An 800 000 time channel data system based on a 32-bit computer was developed in our laboratory [22], which does not have this limitation. This improved system was tied to our ^{252}Cf plasma desorption mass spectrometer and was unfortunately not available for the present experiments. Because of the limited memory, the calibration peaks (generally the H^+ and Na^+ peaks in the positive ion mode) were handled in a different fashion and their arrival times were recorded in a special calibration buffer memory (128 channels for each peak) with 1 ns resolution. This procedure allows for the accurate determination of the centroids of the low mass calibration peaks and the constants required for time-to-mass conversion.

SAMPLE PREPARATION

Samples are inserted into the mass spectrometer on the flat face of a 2 mm diameter stainless steel probe tip. The samples are prepared either by electrospray deposition or by adsorption from solution onto nitrocellulose films. The latter procedure was used for preparation of peptide samples because it produces higher quality mass spectra using smaller amounts of material compared to the electrospray procedure [7,8,12]. Thin films of nitrocellulose (1 $\mu g\,mm^{-2}$) were deposited on the flat face of the probe tip by electrospraying a solution in acetone (1 $\mu g\,\mu l^{-1}$) either over the 3 mm^2 surface or through a mask to give a 0.25 mm $\times$ 2 mm stripe. The peptide solutions (0.1% trifluoroacetic acid) were deposited on the nitrocellulose film using a micropipette. The volume deposited was 1 μl for samples prepared on the whole area of the probe tip and 0.2 μl for those prepared on the nitrocellulose stripe. These peptide solutions were prepared in polypropylene vials just prior to use in order to decrease adsorption losses to the vial walls.

RESULTS AND DISCUSSION

The instrument was found to be highly sensitive for compounds having large secondary ion yields [10]. For example, a quasi-molecular ion peak (m/z 372) was observed with a signal-to-noise ratio of 7:1 from 10^{-15} mol of the cationic dye Crystal Violet electrosprayed on the 3 mm^2 area of the sample insertion probe tip, even though only 7% of the sample area was bombarded in obtaining the mass spectrum. The m/z 372 peak from Crystal Violet had a width of 21 ns (FWHM) at a flight time of 48.4 μs corresponding to a mass resolution of 1100 (FWHM). This resolution was determined largely by the energy spread (ΔE) of the secondary ions and not by the time width of the primary ion pulse, which was determined to be less than 8 ns from the width of the H^+ ion peak. Because the H^+ ion exhibits an extended high energy tail, this time width of 8 ns represents an upper limit to the primary beam pulse width. In principle, the resolution can be increased by simply increasing the acceleration potential and thereby decreasing $\Delta E/E$. However, this strategy could not be used in the present configuration because of the large angle of incidence (70°) of the primary ion beam (see eqn. 2). An electrostatic mirror (not used in the present experiments) would, on the other hand, provide an effective means for decreasing the loss of resolution caused by the energy spreads [23]. Alternatively, the use of a smaller angle of incidence allows for the use of a higher accelerating potential resulting in an improved resolution [14]. This improved resolution is obtained at the cost of a reduction in the bombardment energy at the sample surface for a given primary ion acceleration potential. This latter disadvantage can, in principle, be overcome by incorporation of a primary ion beam carrying negative charge.

We observed that the mass spectra of peptide samples (molecular mass < 6000 u) desorbed from nitrocellulose layers by 30 keV indium ions were very similar to the spectra obtained by ^{252}Cf plasma desorption mass spectrometry [15], in agreement with earlier findings [12]. As predicted, the sensitivity of the present pulsed ion bombardment mass spectrometer was found to be higher than that of our ^{252}Cf plasma desorption mass spectrometer (operated with identical secondary ion energies) for several peptides including arginine vasopressin (molecular mass MM = 1083), a 32-residue synthetic calcitonin analogue (MM = 4576), and bovine insulin (MM = 5733) [15].

The high sensitivity of the instrument for peptides is demonstrated by the mass spectra obtained from samples of arginine vasopressin deposited on the whole area (3 mm^2) of the probe tip. The spectrum for 1.3 pmol of the peptide applied to the tip (Fig. 5a) exhibits an intense $(M + H)^+$ ion at m/z 1084 (calculated m/z = 1084.3). This spectrum was obtained by acquiring data for 3 min. The detection limit for arginine vasopressin is demonstrated in Fig. 5b for a total of 10 fmol applied to the probe tip. The signal-to-noise ratio for the $(M + H)^+$ ion was 3.6:1 for 18 min data acquisition. The mass spectrometric response for the $(M + H)^+$ ion as a function of the amount of arginine vasopressin applied to the probe is plotted in the uppermost curve in Fig. 6. As the applied amount of peptide is increased, the $(M + H)^+$ ion signal increases approximately linearly for amounts between 10 fmol and 10 pmol. For amounts in excess of 10–20 pmol, the response levels off and then decreases. The yield curves for high molecular mass peptides, e.g. bovine insulin (Fig. 6), exhibit a similar behavior. These results are in agreement with those of Jonsson et al. [24] who found that yield maximization occurs when the surface is saturated with the sample, requiring about 1 nmol cm^{-2} of nitrocellulose surface. Because our sample probe area is small (0.03 cm^2), such yield maximization occurs with amounts of sample in the range 10–20 pmol. Peptides with molecular masses above 1000 u often yield doubly protonated intact molecular ions in addition to the singly protonated species. Figure 7 shows the spectrum obtained in 3 min from 1 pmol of bovine insulin applied to the probe tip. The ratio of $(M + 2H)^{2+}$ to $(M + H)^+$ was found to be a strong function of the amount of sample applied (see Fig. 6, bottom curves). Thus at 1 pmol, the $(M + 2H)^{2+}$ peak was almost twice as strong as the $(M + H)^+$ peak. The ratio of $(M + 2H)^{2+}$: $(M + H)^+$ decreases as the amount of sample applied is increased; for 100 pmol the ratio is 0.3:1. A similar dependence of the ratio of $(M + 2H)^{2+}$ to $(M + H)^+$ has previously been observed in ^{252}Cf plasma desorption mass spectrometry [15,24].

To achieve high sensitivity, it is necessary to make complete use of the available sample. Figure 8 shows the intensity of the $(M + H)^+$ ion from arginine vasopressin as a function of the duration of the bombardment by the indium ion beam. One picomole of the peptide was applied uniformly to the

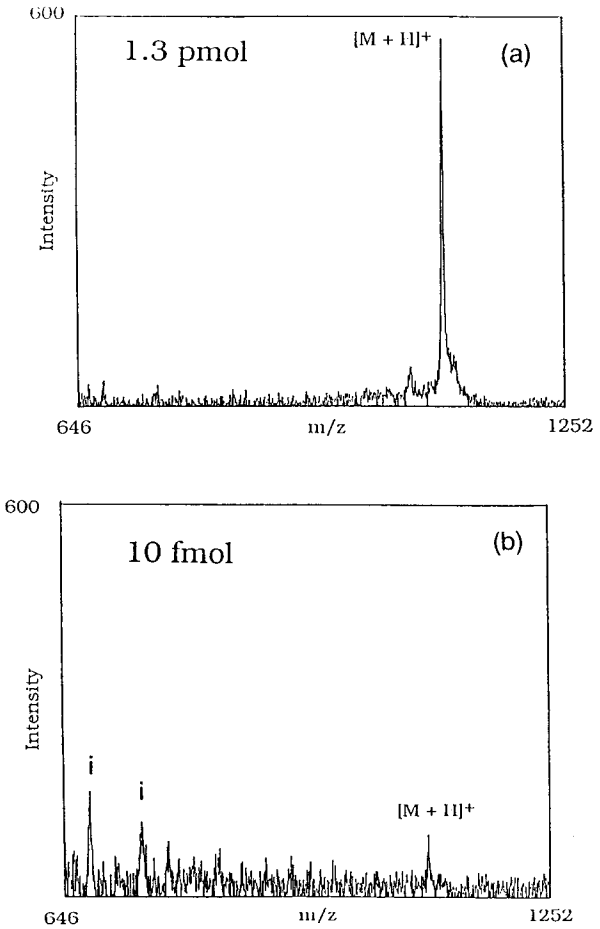

Fig. 5. Mass spectra of arginine vasopressin obtained from: (a) 1.3 pmol applied to 3 mm^2 area probe tip, data acquisition time 3 min; (b) 10 fmol applied to 3 mm^2 area probe tip, data acquisition time 18 min. The peaks denoted by i arise from impurities of unknown origin.

whole area of the probe tip. The signal was observed to decrease exponentially with bombardment time, with a half-life of 22 min. After 90 min bombardment, the response fell to less than 10% of that at the beginning, showing that the sample struck by the beam can be completely utilized. However, only 7% of the applied sample was consumed because only 0.2 mm^2 of the total 3 mm^2 area of the probe tip was struck by the beam. After the 90 min bombardment, the beam was steered to a fresh area of the probe tip whereupon the $(M + H)^+$ signal was observed to increase to a value close to that measured at zero minutes (Fig. 8). This result indicates that higher sensitivities can be obtained if all the available sample were concentrated in the small area swept by the bombarding ion beam.

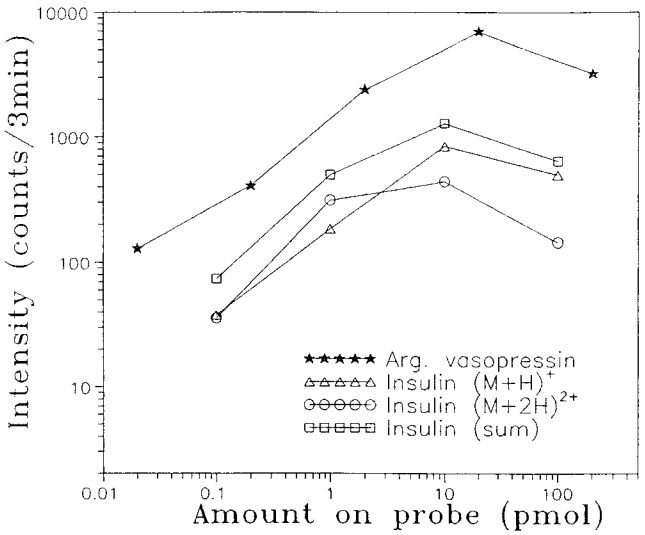

Fig. 6. Plot of mass spectrometric response of arginine vasopressin and bovine insulin as a function of the amount of the peptide applied to the probe tip. The top curve represents the response of the $(M + H)^+$ ion from arginine vasopressin. The bottom curves represent the responses of respectively the $(M + H)^+$ ion, $(M + 2H)^{2+}$ ion, and $[(M + H)^+$ plus $(M + 2H)^{2+}]$ ions from bovine insulin.

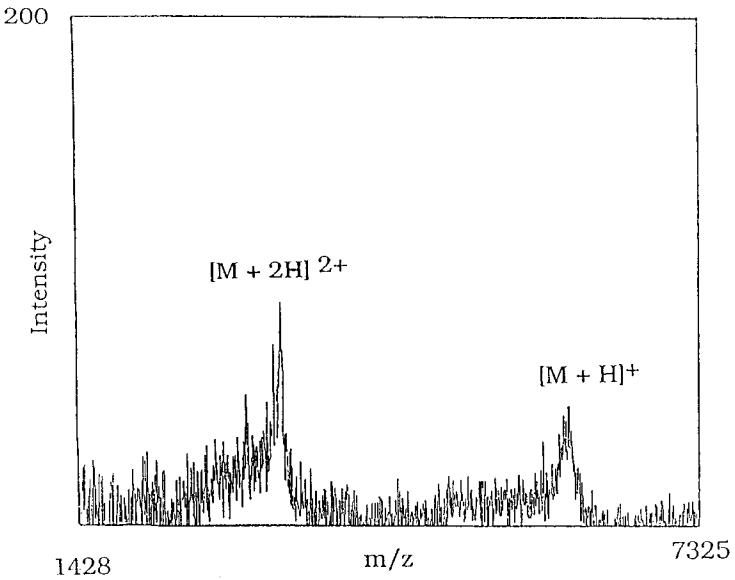

Fig. 7. Partial mass spectrum of bovine insulin obtained from 1 pmol of the protein applied to the probe tip. Data acquisition time 3 min.

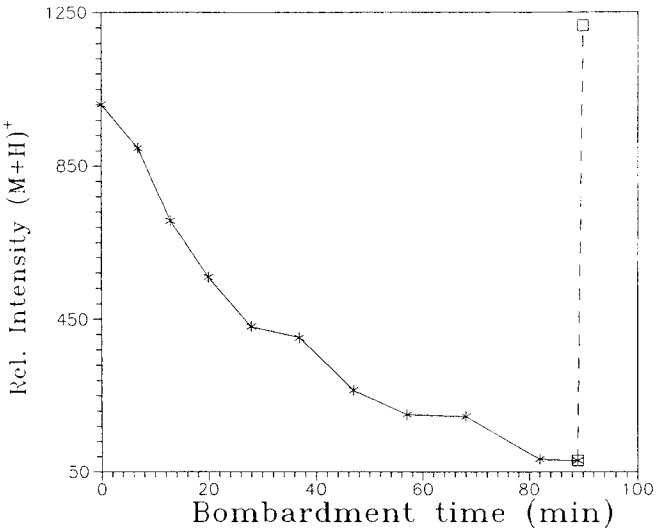

Fig. 8. Plot of the intensity of the $(M + H)^+$ ion from arginine vasopressin as a function of the bombardment time. The signal decreased exponentially with a half life of about 22 min. After a 90 min bombardment the intensity falls to less than 10% of the initial value. Sample is consumed only in the area bombarded by the beam. Moving the primary ion beam to a different spot on the probe tip, after the 90 min bombardment, restores the $(M + H)^+$ ion intensity to close to its original value.

To achieve a further increase in sensitivity, the peptides were therefore applied to a small fraction of the probe tip area. The sample was restricted to this small area by producing a nitrocellulose stripe (0.25 mm × 2 mm) on the probe tip and then applying the peptide exclusively to the area covered by the nitrocellulose stripe. Figure 9 shows a comparison of the spectrum obtained from 100 fmol of arginine vasopressin applied to the whole area of the probe tip with the spectrum obtained for the same amount applied to the nitrocellulose stripe. A three-fold increase in the intensity of the $(M + H)^+$ ion peak was observed for the sample applied to the smaller area stripe, demonstrating the efficiency of the strategy. The increase was a factor of two lower than that predicted on the basis of the increased surface concentration of sample, implying that losses probably occurred during the handling of the small volume (0.2 μl) samples. Figure 10 compares the $(M + H)^+$ ion yield as a function of the amount of arginine vasopressin for the case of the peptide deposited on the whole area of the probe tip versus that for the peptide deposited on the stripe. In the former case, the signal increases approximately linearly for amounts up to 10 pmol as described earlier. For the sample deposited on the stripe, on the other hand, the signal saturates at 1–2 pmol as predicted by the six-fold smaller area of the stripe. Such yield maximization at the 1–2 pmol level was also observed with the synthetic analogue of calcitonin and bovine insulin deposited on the stripe.

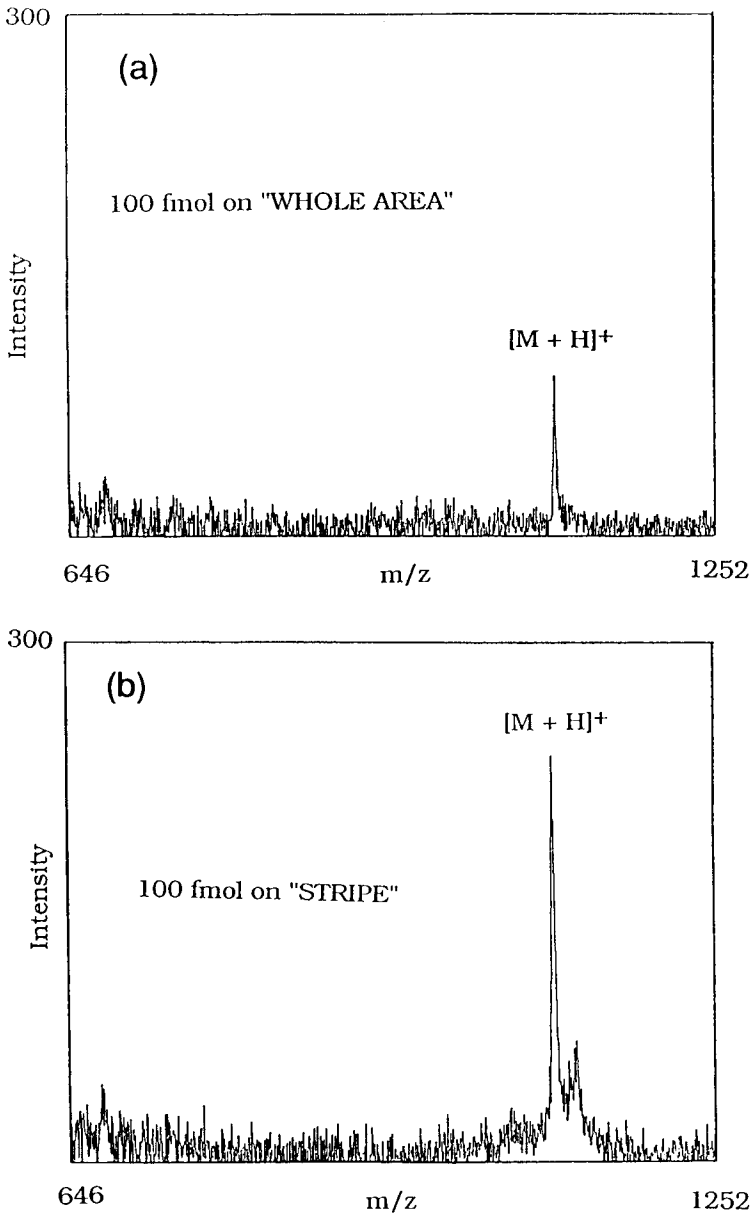

Fig. 9. Comparison of the mass spectra of arginine vasopressin obtained under similar conditions from: (a) 100 fmol of material applied to the whole area; (b) versus the same amount applied to the smaller area nitrocellulose stripe.

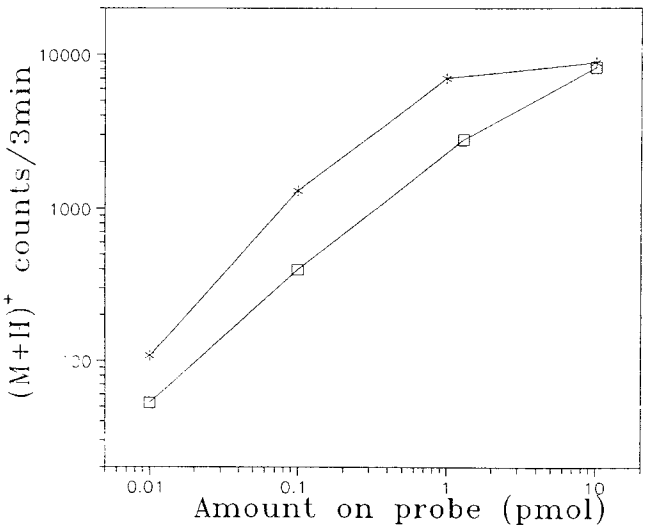

Fig. 10. Comparison of the $(M + H)^+$ ion yield from arginine vasopressin as a function of the amount applied to the whole area of the tip versus the same amount applied to the nitrocellulose stripe. In the case of the stripe, the signal levels off at 1–2 pmol of material applied.

CONCLUSION

Our goal of designing an instrument with an optimum sensitivity in the low picomole range for peptides with molecular masses up to 6000 u was accomplished by efficient utilization of sample in the described pulsed ion bombardment TOF mass spectrometer. The strategy for achieving this sensitivity is to concentrate the available peptide in a small surface area and to utilize most of the sample by bombardment with an intense tightly focussed ion beam. The resolution of the instrument was limited ($\approx$ 1000 FWHM) by the requirement that the secondary ion energy be less than 3.5 keV. Higher resolutions are attainable by incorporation of an electrostatic mirror or by the use of a smaller angle of incidence for the primary ion beam. Reasonably high quality mass spectra were obtained from picomole amounts of peptides in times of 3–30 min.

ACKNOWLEDGMENTS

We thank Dr. Frank H. Field for his advice and encouragement and Mr. Louis I. Grace for technical help concerning the CAMAC instrumentation. This work was supported in part by a grant from the Division of Research Resources, National Institute of Health (RR00862).

REFERENCES

1 B. Sundquist and R.D. Macfarlane, Mass Spectrom. Rev., 4 (1985) 421.
2 K.G. Standing, R. Beavis, G. Bolback, W. Ens, D.E. Main and B. Schueler, SIMS V, Springer Ser. Chem. Phys., 44 (1986) 476.
3 W. Lange, D. Greifendorf, D. Van Leyne, E. Niehuis and A. Benninghoven, Ion Formation from Organic Solids III, Springer Proc. Physics, 9 (1986) 67.
4 C.J. McNeal, R.D. Macfarlane and E.L. Thurston, Anal. Chem., 51 (1979) 2036.
5 A. Benninghoven, E. Niehus, T. Friese, D. Greifendorf and P. Steffens, Org. Mass Spectrom., 19 (1984) 346.
6 A. Eicke and A. Benninghoven, in Ion Formation from Organic Solids III, Springer Ser. Chem. Phys., 9 (1986) 56.
7 G. Jonsson, A. Hedin, P. Håkansson, B.U.R. Sundquist, G. Save, P. Roepstorff, K.E. Johansson, I. Kaminsky and M. Lindberg, Anal. Chem., 58 (1986) 1084.
8 B.T. Chait, Int. J. Mass Spectrom. Ion Processes, 78 (1987) 237.
9 B.T. Chait, Int. J. Mass Spectrom. Ion. Processes, 92 (1989) 297.
10 B.T. Chait and F.H. Field, Proc. 32nd ASMS Conf. Mass Spectrometry and Allied Topics, San Antonio, TX, May 1984, pp. 237, 238.
11 W. Ens, K.G. Standing, B.T. Chait and F.H. Field, Anal. Chem., 53 (1981) 1241.
12 F. Lafortune, R. Beavis, X. Tang, K.G. Standing and B.T. Chait, Rapid Commun. Mass Spectrom., 1 (1987) 114.
13 W. Ens, D.E. Main, K.G. Standing and B.T. Chait, Anal. Chem., 60 (1988) 1494.
14 B.T. Chait and K.G. Standing, Int. J. Mass Spectrom. Ion Phys., 40 (1981) 185.
15 V. Katta, L.I. Grace, T. Chaudhary and B.T. Chait, Proc. 36th ASMS Conf. Mass Spectrometry and Allied Topics, San Francisco, CA, June 1988, pp. 413, 414.
16 R.D. Macfarlane and D.F. Torgerson, Int. J. Mass Spectrom. Ion Phys., 21 (1976) 81.
17 A. Wagner and T.M. Hall, J. Vac. Sci. Technol., 16 (1979) 1871.
18 J.F. Mahoney, A.Y. Yakihu, H.L. Daley, R.D. Moore and J.J. Perel, Appl. Phys., 40 (1969) 5101.
19 T.K. Fowler and W.M. Good, Nucl. Instrum. Methods, 7 (1960) 242.
20 J.V. Kane, M.A. Fl-Wahab, J. Lowe and C.L. McClelland, Proc. Int. Conf. Nuclear Electronics, 3 (1962) 345.
21 W. Szymczak and K. Wittmack, in A. Benninghoven, C. A. Evans, K. D. McKeegan, H. A. Storms and H. W. Werner (Eds.), Secondary Ion Mass Spectrometry SIMS VII, Wiley, Chichester, 1990, pp. 65–68.
22 L.I. Grace, B.T. Chait and F.H. Field, Biomed. Environ. Mass Spectrom., 14 (1987) 295.
23 X. Tang, R. Beavis, W. Ens, F. Lafortune, B. Schueler and K.G. Standing, Int. J. Mass Spectrom. Ion Processes, 85 (1988) 43.
24 G. Jonsson, A. Hedin, P. Håkansson and B.U.R. Sundquist, Rapid Commun. Mass Spectrom., 2 (1988) 154.